

Cross Sections for Leptophobic Topcolor Z' decaying to top-antitop

Robert M. Harris,¹ Supriya Jain²

¹*Fermi National Accelerator Laboratory*
²*State University of New York at Buffalo*

(Dated: April 15, 2012)

We present numerical calculations of the production cross section of a heavy Z' resonance in hadron-hadron collisions with subsequent decay into top-antitop pairs. In particular, we consider the leptophobic topcolor Z' discussed under Model IV of hep-ph/9911288 which has predicted cross sections large enough to be experimentally accessible at the Fermilab Tevatron and the Large Hadron Collider at CERN. Cross sections are presented for various Z' widths, in $p\bar{p}$ collisions at $\sqrt{s} = 2$ TeV, and in pp collisions at $\sqrt{s} = 7, 8, 10$ and 14 TeV.

CONTENTS

I. Introduction	1
II. Cross Section for Z' Production and Decay	1
III. Cross sections at the Tevatron	2
IV. Cross sections at the LHC	2
V. Conclusions	3
VI. Acknowledgments	3
References	4

I. INTRODUCTION

Electroweak symmetry breaking is a cornerstone for our understanding of particle physics. However, despite the spectacular phenomenological success of the Standard Model (SM), the fundamental mechanism of electroweak symmetry breaking remains a mystery. Various new models have been proposed to explain this mechanism. One such class of models is based upon topcolor [1, 2] which can generate a large top-quark mass. The topcolor model also predicts a Z' [3].

The physics in production and decay of the Z' are discussed in Ref. [3] under different model assumptions. In this paper, we consider the Z' from Model IV which represents a novel class and has predicted cross sections large enough to be experimentally accessible at hadron colliders at the Fermilab Tevatron and the Large Hadron Collider (LHC) at CERN. Such Z' resonances couple strongly only to the first and third generation of quarks, and have no significant couplings to the leptons. They are, therefore, leptophobic and topophylic.

The leptophobic topcolor Z' decaying to $t\bar{t}$ has been searched for at both the Tevatron [4–6] and the LHC [7]. The Tevatron searches used a previous calculation of the Z' cross section [3]. The LHC search conducted by the CMS collaboration have used the cross section calculation presented here to set limits on the Z' mass. This

article is primarily intended to document that Z' cross section used for a pp collision energy of $\sqrt{s} = 7$ TeV. For current and future LHC searches, we present the Z' cross section at the current LHC pp collision energy of $\sqrt{s} = 8$ TeV and the potential future collision energies of 10 and 14 TeV. We also present the cross section in $p\bar{p}$ collisions at $\sqrt{s} = 2$ TeV for comparison with Tevatron searches.

II. CROSS SECTION FOR Z' PRODUCTION AND DECAY

The total lowest-order cross section for a Z' produced in hadron collisions and decaying into top-antitop pairs from Model IV discussed above, is given by:

$$\sigma_{Z'} \times \text{B}(Z' \rightarrow t\bar{t}) \equiv \sigma = \int_0^\infty \frac{d\sigma}{dm} dm \quad (1)$$

where $d\sigma/dm$, the differential cross section at $t\bar{t}$ invariant mass m , is given by

$$\frac{d\sigma}{dm} = \frac{2}{m} \int_{-\ln(\sqrt{s}/m)}^{\ln(\sqrt{s}/m)} dy_b \tau \mathcal{L}(x_{h1}, x_{h2}) \hat{\sigma}(q\bar{q} \rightarrow Z' \rightarrow t\bar{t}). \quad (2)$$

Here $\hat{\sigma}(q\bar{q} \rightarrow Z' \rightarrow t\bar{t})$ is the parton-level subprocess cross section. The kinematic variable τ is related to the initial-state parton fractional momenta inside the first hadron x_{h1} and second hadron x_{h2} by $\tau = x_p x_{\bar{p}} = m^2/s$. The boost of the partonic system y_b is given by $y_b = (1/2) \ln(x_{h1}/x_{h2})$. The partonic “luminosity function” is just the product of parton distribution functions:

$$\mathcal{L}(x_{h1}, x_{h2}) = q(x_{h1}, \mu) \bar{q}(x_{h2}, \mu) + \bar{q}(x_{h1}, \mu) q(x_{h2}, \mu) \quad (3)$$

where $q(x, \mu)$ ($\bar{q}(x, \mu)$) is the parton distribution function of a quark (anti-quark) evaluated at fractional momenta x and renormalization scale μ .

The parton-level subprocess cross section, $\hat{\sigma}(q\bar{q} \rightarrow Z' \rightarrow t\bar{t})$, for a leptophobic, b_r -phobic, and topophylic, Z' is given by:

$$\hat{\sigma} \rightarrow \frac{9\alpha^2\pi}{16\cos^4\theta_W} \cot^4\theta_H \times (2 \text{ for initial state } u + \bar{u};, (1) \text{ for initial } d + \bar{d}) \times \left[2 \times \beta(1 + \frac{1}{3}\beta^2) + \beta(1 - \beta^2) \right] \left[\frac{s}{(\hat{s} - M_{Z'}^2)^2 + \hat{s}\Gamma_{Z'}^2} \right] \theta(\hat{s} - 4m_t^2), \quad (4)$$

where $\cot^4\theta_H$ can be obtained from the total decay-width of the resonance [8]:

$$\Gamma_{Z'} = \frac{\alpha \cot^2\theta_H M_{Z'}}{8\cos^2\theta_W} \left[\sqrt{1 - \frac{4m_t^2}{M_{Z'}^2}} \left(2 + 4\frac{m_t^2}{M_{Z'}^2} \right) + 4 \right]. \quad (5)$$

The subprocess cross section in Eq. 4 is for spin and color summing on both initial and final state legs, while most parton distributions assume spin and color averaged on the initial-state legs and spin and color summing on the final-state legs. Therefore, the subprocess cross section given by Eq. 4 must be multiplied by a factor of

$$\left(\frac{1}{\text{spins}} \right)^2 \left(\frac{1}{\text{colors}} \right)^2 = \left(\frac{1}{2} \right)^2 \left(\frac{1}{3} \right)^2 = \frac{1}{36} \quad (6)$$

when used with parton distributions from PDFLIB [9] and other standard sources. We have taken this into account when calculating the cross section. We have also used $m_t = 172.5 \text{ GeV}/c^2$, and $\cos^2\theta_W = .768$. For a default parton distribution set we have chosen CTEQ6L [10]. This is a modern parton distribution set appropriate for leading-order calculations and is available in PDFLIB [9]. For a default renormalization scale we choose $\mu = m/2$, half the $t\bar{t}$ invariant mass. This scale has the benefit that it reduces to the usual $\mu = m_t$ at top production threshold, but also increases with increasing $t\bar{t}$ invariant mass. With these choices, the total cross section for the production of a leptophobic and topophilic Z' and its subsequent decay into $t\bar{t}$ pairs is presented in Sections III and IV for the Tevatron and the LHC.

III. CROSS SECTIONS AT THE TEVATRON

We calculate numerically the lowest order cross section for the process $p\bar{p} \rightarrow Z' \rightarrow t\bar{t}$ at the Tevatron at $\sqrt{s} = 2 \text{ TeV}$, using Eq. 1 and taking into account the spin-color factor in Eq. 6. The only remaining parameter of the topcolor model that affects the cross section is the mixing angle $\cot^2\theta_H$, or equivalently the width $\Gamma_{Z'}$ which is related to it. We calculate the cross section for different choices of $\Gamma_{Z'}$, equal to 1.2% and 2% of $M_{Z'}$, both of which qualify as narrow resonances at the Tevatron. The integration in Eq. 1 is performed using the full available phase space of $2m_t < m < \sqrt{s}$. The results are tabulated in Table I and displayed in Fig. 1.

IV. CROSS SECTIONS AT THE LHC

We perform the numerical calculation of the lowest order cross section for the process $pp \rightarrow Z' \rightarrow t\bar{t}$ at the

TABLE I. Cross sections at the Tevatron at $\sqrt{s} = 2 \text{ TeV}$ for $\sigma_{Z'} B(Z' \rightarrow t\bar{t})$ at different Z' masses and widths.

$M_{Z'}$ [GeV/ c^2]	$\sigma_{Z'} B(Z' \rightarrow t\bar{t})$ [pb]	
	$\Gamma_{Z'}/M_{Z'} = 0.012$	$\Gamma_{Z'}/M_{Z'} = 0.02$
400.0	9.49	15.62
500.0	4.25	7.03
600.0	1.77	2.95
700.0	0.705	1.18
750.0	0.435	0.735
800.0	0.273	0.462
900.0	0.103	0.178
1000.0	3.80E-02	6.76E-02
1100.0	1.33E-02	2.50E-02
1200.0	4.75E-03	9.81E-03

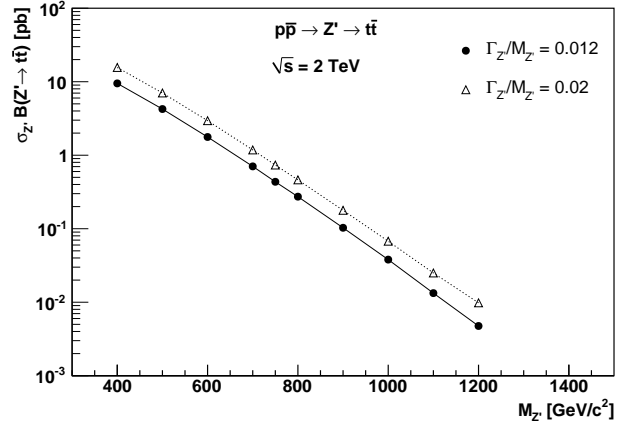


FIG. 1. Cross sections at the Tevatron at $\sqrt{s} = 2 \text{ TeV}$, for $\sigma_{Z'} B(Z' \rightarrow t\bar{t})$, with different choices of the resonance width.

LHC for different values of \sqrt{s} between 7 – 14 TeV, using Eq. 1 and taking into account the spin-color factor in Eq. 6. We calculate the cross section for different choices of $\Gamma_{Z'}$, equal to 1%, 1.2%, 2%, and 10% of $M_{Z'}$. The first three widths qualify as narrow resonance at the LHC, and the integration in Eq. 1 is performed using the full available phase space of $2m_t < m < \sqrt{s}$. The integration for $\Gamma_{Z'} = 10\% M_{Z'}$ is performed using the mass interval $M_{Z'} - 3\Gamma_{Z'} < m < M_{Z'} + 3\Gamma_{Z'}$ in order to sample better the cross section around the peak of the resonance. The results are tabulated in Tables II-V, and displayed in Figs. 2-5.

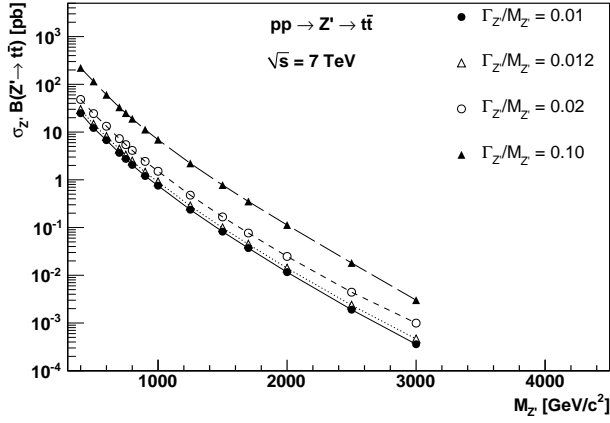


FIG. 2. Cross sections at the LHC at $\sqrt{s} = 7$ TeV, for $\sigma_{Z'} B(Z' \rightarrow t\bar{t})$, with different choices of the resonance width.

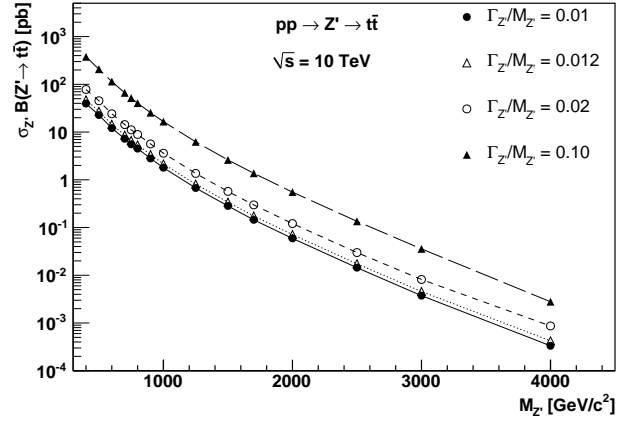


FIG. 4. Cross sections at the LHC at $\sqrt{s} = 10$ TeV, for $\sigma_{Z'} B(Z' \rightarrow t\bar{t})$, with different choices of the resonance width.

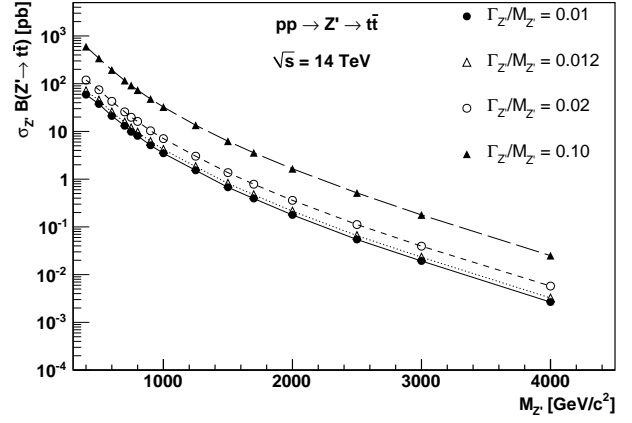


FIG. 5. Cross sections at the LHC at $\sqrt{s} = 14$ TeV, for $\sigma_{Z'} B(Z' \rightarrow t\bar{t})$, with different choices of the resonance width.

V. CONCLUSIONS

We have presented cross section calculations of the leptophobic topcolor Z' decaying to $t\bar{t}$. These calculations update the results presented in Ref. [3] for the Tevatron, by both fixing an error in the reported width of the leptophobic topcolor Z' , and using $m_t = 172.5$ GeV/c² and CTEQ6L parton distributions in an improved calculation procedure. This note documents the first calculations of the cross section for a leptophobic topcolor Z' at the LHC.

VI. ACKNOWLEDGMENTS

We thank Chris Hill for sending us the correction to the equation for the topcolor Z' width, found by James Ferrando and Mads Frandsen. We also thank Jan Stegmann and Ia Iashvili for several useful discussions.

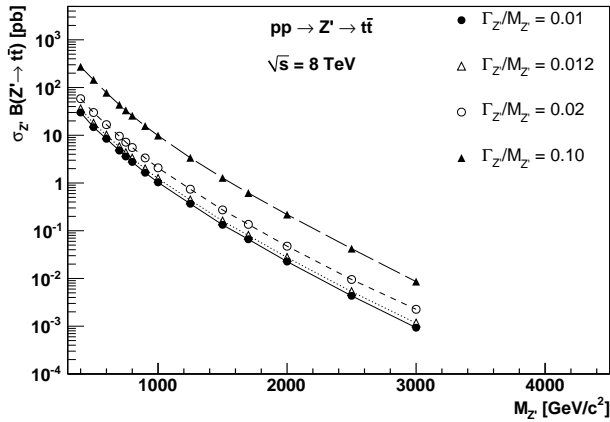


FIG. 3. Cross sections at the LHC at $\sqrt{s} = 8$ TeV, for $\sigma_{Z'} B(Z' \rightarrow t\bar{t})$, with different choices of the resonance width.

-
- [1] C. T. Hill *Phys. Lett.* **B266** 419, (1991);
Phys. Lett. **B345** 483 (1995).
 - [2] C. T. Hill and S. Parke, *Phys. Rev.* **D49** 4454 (1994).
 - [3] R. M. Harris, C. T. Hill, S. J. Parke, “Cross Section for Topcolor Z' decaying to top-antitop”, Fermilab-FN-687, arXiv:hep-ph/9911288 (1999).
 - [4] CDF Collaboration, *Phys. Rev.* **D77** 051102 (2008).
 - [5] CDF Collaboration, *Phys. Rev. Lett.* **100** 231801 (2008).
 - [6] D0 Collaboration, *Phys. Rev.* **D85** 051101 (2012).
 - [7] CMS Collaboration, “Search for anomalous $t\bar{t}$ production in the highly-boosted all-hadronic final state”, CERN-PH-EP-2012-077, arXiv:1204.2488 (2012).
 - [8] James Ferrando, Mads Frandsen, and Chris Hill informed us that Eq. 28 of Ref. [3] had a mistake which also affected Eq. 32 and Eq. 33: the last term in the parenthesis of Eq. 28 should be multiplied by $+6f_1$ instead of $-3f_1$. Our Eq. 5 replaces Eq. 33 in Ref. [3], correcting for the mistake.
 - [9] M. R. Whalley, D. Bourilkov, R. C. Group, “The Les Houches accord PDFs (LHAPDF) and LHAGLUE”, Contributed to HERA and the LHC: A Workshop on the Implications of HERA and LHC Physics, Hamburg, Germany, 21-24 Mar 2005, arXiv:hep-ph/0508110; <http://projects.hepforge.org/lhapdf>
 - [10] H. L. Lai *et al.*, *Phys. Rev.* **D55**, 1280 (1997).

TABLE II. Cross sections at the LHC at $\sqrt{s} = 7$ TeV for $\sigma_{Z'}\text{B}(Z' \rightarrow t\bar{t})$ at different Z' masses and widths.

$M_{Z'}$ [GeV/c ²]	$\sigma_{Z'}\text{B}(Z' \rightarrow t\bar{t})$ [pb]			
	$\Gamma_{Z'}/M_{Z'} = 0.01$	$\Gamma_{Z'}/M_{Z'} = 0.012$	$\Gamma_{Z'}/M_{Z'} = 0.02$	$\Gamma_{Z'}/M_{Z'} = 0.10$
400.0	24.82	29.61	48.24	220.92
500.0	12.17	14.61	24.37	115.29
600.0	6.76	8.07	13.27	60.37
700.0	3.66	4.39	7.29	33.07
750.0	2.74	3.28	5.45	24.95
800.0	2.05	2.47	4.13	19.00
900.0	1.20	1.44	2.43	11.27
1000.0	0.753	0.905	1.51	6.91
1250.0	0.236	0.283	0.477	2.21
1500.0	8.20E-02	9.87E-02	0.167	0.777
1700.0	3.71E-02	4.48E-02	7.67E-02	0.352
2000.0	1.16E-02	1.41E-02	2.48E-02	0.113
2500.0	1.90E-03	2.36E-03	4.42E-03	1.81E-02
3000.0	3.59E-04	4.64E-04	9.95E-04	3.01E-03

TABLE III. Cross sections at the LHC at $\sqrt{s} = 8$ TeV for $\sigma_{Z'}\text{B}(Z' \rightarrow t\bar{t})$ at different Z' masses and widths.

$M_{Z'}$ [GeV/c ²]	$\sigma_{Z'}\text{B}(Z' \rightarrow t\bar{t})$ [pb]			
	$\Gamma_{Z'}/M_{Z'} = 0.01$	$\Gamma_{Z'}/M_{Z'} = 0.012$	$\Gamma_{Z'}/M_{Z'} = 0.02$	$\Gamma_{Z'}/M_{Z'} = 0.10$
400.0	29.97	35.77	58.46	271.98
500.0	14.79	17.82	29.98	145.06
600.0	8.42	10.08	16.70	77.71
700.0	4.78	5.74	9.57	43.59
750.0	3.59	4.31	7.17	33.29
800.0	2.76	3.32	5.54	25.67
900.0	1.64	1.98	3.35	15.63
1000.0	1.03	1.24	2.08	9.84
1250.0	0.367	0.441	0.742	3.37
1500.0	0.133	0.160	0.273	1.28
1700.0	6.62E-02	7.99E-02	0.136	0.616
2000.0	2.26E-02	2.75E-02	4.75E-02	0.218
2500.0	4.33E-03	5.30E-03	9.52E-03	4.21E-02
3000.0	9.30E-04	1.16E-03	2.26E-03	8.59E-03

TABLE IV. Cross sections at the LHC at $\sqrt{s} = 10$ TeV for $\sigma_{Z'}B(Z' \rightarrow t\bar{t})$ at different Z' masses and widths.

$M_{Z'}$ [GeV/c ²]	$\sigma_{Z'}B(Z' \rightarrow t\bar{t})$ [pb]			
	$\Gamma_{Z'}/M_{Z'} = 0.01$	$\Gamma_{Z'}/M_{Z'} = 0.012$	$\Gamma_{Z'}/M_{Z'} = 0.02$	$\Gamma_{Z'}/M_{Z'} = 0.10$
400.0	39.51	47.28	77.96	377.58
500.0	22.69	27.22	45.29	207.45
600.0	12.08	14.51	24.20	114.59
700.0	7.23	8.64	14.35	66.36
750.0	5.53	6.66	11.14	51.51
800.0	4.50	5.38	8.91	40.38
900.0	2.80	3.37	5.65	25.44
1000.0	1.79	2.15	3.61	16.59
1250.0	0.673	0.811	1.36	6.24
1500.0	0.283	0.340	0.571	2.61
1700.0	0.145	0.175	0.298	1.37
2000.0	5.92E-02	7.12E-02	0.121	0.552
2500.0	1.44E-02	1.74E-02	2.99E-02	0.135
3000.0	3.74E-03	4.57E-03	8.16E-03	3.57E-02
4000.0	3.33E-04	4.24E-04	8.67E-04	2.79E-03

TABLE V. Cross sections at the LHC at $\sqrt{s} = 14$ TeV for $\sigma_{Z'}B(Z' \rightarrow t\bar{t})$ at different Z' masses and widths.

$M_{Z'}$ [GeV/c ²]	$\sigma_{Z'}B(Z' \rightarrow t\bar{t})$ [pb]			
	$\Gamma_{Z'}/M_{Z'} = 0.01$	$\Gamma_{Z'}/M_{Z'} = 0.012$	$\Gamma_{Z'}/M_{Z'} = 0.02$	$\Gamma_{Z'}/M_{Z'} = 0.10$
400.0	58.83	70.86	119.29	597.95
500.0	37.60	45.08	74.65	339.69
600.0	21.05	25.43	42.73	194.07
700.0	13.12	15.66	25.69	116.34
750.0	9.80	11.81	19.80	91.89
800.0	8.05	9.68	16.19	73.33
900.0	5.12	6.16	10.31	47.91
1000.0	3.48	4.19	7.07	32.44
1250.0	1.53	1.83	3.03	13.47
1500.0	0.675	0.814	1.37	6.24
1700.0	0.393	0.471	0.784	3.57
2000.0	0.178	0.214	0.360	1.65
2500.0	5.44E-02	6.57E-02	0.112	0.515
3000.0	1.93E-02	2.32E-02	3.95E-02	0.178
4000.0	2.66E-03	3.24E-03	5.76E-03	2.50E-02